

## Interaction of Poly(glycoamidoamine) DNA Delivery Vehicles with Cell-Surface Glycosaminoglycans Leads to Polyplex Internalization in a Manner Not Solely Dependent on Charge

Patrick M. McLendon,<sup>†</sup> Daniel J. Buckwalter, Erica M. Davis, and  
Theresa M. Reineke\*

*Macromolecules and Interfaces Institute, Department of Chemistry, Virginia Tech,  
Blacksburg, Virginia 24061*

Received April 23, 2010; Revised Manuscript Received June 23, 2010; Accepted July 6, 2010

**Abstract:** Understanding the mechanisms of cellular internalization is necessary for rational design of efficient polymers for DNA delivery. In this paper, we present evidence that poly(glycoamidoamine) (PGAA)–DNA complexes (polyplexes) interact with cell-surface glycosaminoglycans (GAGs) in a manner that is not solely dependent on charge. The presence of GAGs appears to be necessary for efficient cellular uptake, as polyplex internalization was decreased in GAG-deficient CHO (pgsA-745) cells. However, uptake was nearly unaffected in cells deficient only in heparan sulfate. Internalization of PGAA polyplexes appears to be dependent on GAG sulfation in mammalian cell lines, yet the PGAA polymers are decomplexed from pDNA by high concentrations of GAGs in a charge-independent manner. This finding suggests that interactions between the carbohydrates on the polymer and GAGs may contribute to polyplex binding. Quartz crystal microbalance studies support the findings that relative PGAA polyplex–GAG binding affinities are also not completely mediated by charge. As measured by dynamic light scattering and TEM, GAGs appear to accumulate on the surface of polyplexes without disrupting them at a lower concentration, which may stimulate cellular internalization due to close interactions between the polyplexes and the GAGs. Gel electrophoresis and fluorescence measurements of an intercalating dye suggest that polyplex interaction with GAGs can induce dissociation, which could represent a potential pDNA release mechanism. These results imply that similar interactions may occur on cell surfaces, and strongly supports the hypothesis that GAGs function as cell surface receptors for polyplexes formed with PGAA vehicles.

**Keywords:** Poly(glycoamidoamine); glycosaminoglycan; proteoglycan; polyplex; cellular internalization

### Introduction

Nucleic acid delivery has emerged as a potential therapeutic strategy that promises a broad impact in disease treatment.<sup>1</sup> Nonviral vehicles have been developed as

alternative polynucleotide carriers to virus-based transport systems. These versatile vehicles are able to carry different nucleic acid types, can be readily modified for different targets, and can be optimized to circumvent immunogenic responses.<sup>2</sup> Synthetic delivery vehicles can also be easily modified to increase residency in the bloodstream,<sup>3</sup> facilitate

\* Address correspondence to this author. Mailing address: 2107 Hahn Hall, Blacksburg, VA 24061. Phone: 540-231-7011. Fax: 540-231-3255. E-mail: treineke@vt.edu.

<sup>†</sup> Current address: Division of Molecular Cardiovascular Biology, Cincinnati Children's Hospital Medical Center, Cincinnati, OH 45229.

(1) Verma, I. M.; Somia, N. Gene Therapy - Promises, Problems, and Prospects. *Nature* **1997**, 389, 239–242.

(2) Mintzer, M. A.; Simanek, E. E. Nonviral Vectors for Gene Delivery. *Chem. Rev.* **2009**, 109, 259–302.

cell specific targeting,<sup>4</sup> and permit monitoring of delivery *in vitro* and *in vivo*,<sup>5</sup> which make synthetic systems attractive candidates for site-specific delivery. Despite these attributes, development of highly efficacious nonviral nucleic acid delivery vehicles has been hindered by an incomplete understanding of the molecular mechanisms of delivery at the cellular level.

Several subclasses of nonviral vehicles have been developed and studied, including those based on cationic polymers, lipids, and peptides.<sup>2</sup> The physical and chemical structures of these carriers vary widely and likely dictate interactions with biomolecules surrounding and within the cellular environment. Indeed, polyplex binding with the cell surface, internalization, and intracellular trafficking are certainly functions of chemical functionality, and understanding how the chemical structure influences these biological pathways is crucial for rational vehicle design. While studies have been completed to understand the trafficking mechanisms of some nonviral nucleic acid delivery vehicles,<sup>2,6–8</sup> investigation and comparison of these mechanisms as a function of subtle chemical alterations is essential for the development and refinement of the next generation of carriers that offer control over cell-specific entry, intracellular localization, and proper release kinetics.

Toward this end, we have developed a series of cationic glycopolymers, termed poly(glycoamidoamine)s (PGAAs), for use as nucleic acid transport vehicles (Figure 1).<sup>9–11</sup> These short polymers incorporate a carbohydrate moiety into a polyethyleneamine backbone. Through a series of systematic studies, we have determined that the presence of four

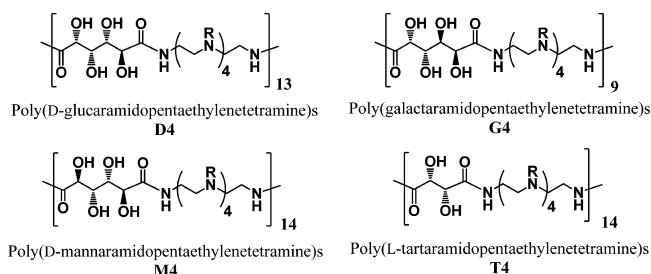


**Figure 1.** Chemical structures of the poly(glycoamidoamine) (PGAA) nucleic acid delivery polymers. Polymers consist of a carbohydrate monomer [galactarate (G), glucarate (D), mannarate (M), and tartarate (T)] and a polyethyleneamine monomer containing four protonatable secondary amines. The degrees of polymerization are as indicated. R = H or site of branching. Figure was adapted from Liu et al.<sup>10</sup>

secondary amines in each repeat unit leads to the most efficient pDNA binding and the highest transgene delivery with mammalian cells in a nontoxic manner.<sup>12,13</sup> These vehicles are able to enter the cell through multiple endocytic routes, then undergo various intracellular trafficking mechanisms; we have found that a primary uptake route for nuclear delivery and gene expression with PGAA polyplexes is via caveolae/raft-mediated endocytosis.<sup>14</sup> We have demonstrated that these polymers can degrade under physiological conditions, which likely influences the ability of the vehicle to traffic and release the nucleic acid cargo, and can affect the overall kinetics of delivery.<sup>15</sup>

In the current study, we seek to understand the nature of PGAA-based polyplex interactions with cell-surface glycosaminoglycans (GAGs), which coat cells and play a major role in triggering cell entry. The GAGs are linear polysaccharides of a repeating disaccharide motif that exist on cell surfaces, forming a major component of the extracellular matrix (Figure S1 in the Supporting Information). They primarily exist bound to transmembrane or glycosylphosphatidylinositol-anchored proteins forming structures known as proteoglycans (PGs). In mammalian tissues, GAGs play important roles in cell migration, differentiation, and cell–cell communication, including the binding and sequestration of

(3) Pun, S. H.; Davis, M. E. Development of a Nonviral Gene Delivery Vehicle for Systemic Application. *Bioconjugate Chem.* **2002**, *13*, 630–639.

(4) Zanta, M. A.; Boussif, O.; Adib, A.; Behr, J. P. In vitro gene delivery to hepatocytes with galactosylated polyethylenimine. *Bioconjugate Chem.* **1997**, *8* (6), 839–844.

(5) Bryson, J. M.; Fichter, K. M.; Chu, W.-J.; Lee, J.-H.; Li, J.; Madsen, L. A.; McLendon, P. M.; Reineke, T. M. Polymer beacons for luminescence and magnetic resonance imaging of DNA delivery. *Proc. Natl. Acad. Sci. U.S.A.* **2009**, *106* (40), 16913–16918.

(6) Khalil, I. A.; Kogure, K.; Akita, H.; Harashima, H. Uptake Pathways and Subsequent Intracellular Trafficking in Nonviral Gene Delivery. *Pharmacol. Rev.* **2006**, *58* (1), 32–45.

(7) Medina-Kauwe, L. K.; Xie, J.; Hamm-Alvarez, S. Intracellular Trafficking of Nonviral Vectors. *Gene Ther.* **2005**, *12*, 1734–1751.

(8) Midoux, P.; Breuzard, G.; Gomes, J. P.; Pichon, C. Polymer-based Gene Delivery: A Current Review on the Uptake and Intracellular Trafficking Pathways of Polyplexes. *Curr. Gene Ther.* **2008**, *8*, 335–352.

(9) Liu, Y.; Reineke, T. M. Hydroxyl Stereochemistry and Amine Number within Poly(glycoamidoamine)s Affect Intracellular DNA Delivery. *J. Am. Chem. Soc.* **2005**, *127*, 3004–3015.

(10) Liu, Y.; Reineke, T. M. Poly(glycoamidoamine)s for Gene Delivery: Stability of Polyplexes and Efficacy with Cardiomyoblast Cells. *Bioconjugate Chem.* **2006**, *17* (1), 101–108.

(11) Liu, Y.; Wenning, L.; Lynch, M.; Reineke, T. M. New Poly(D-glucaramidoamine)s Induce DNA Nanoparticle Formation and Efficient Gene Delivery into Mammalian Cells. *J. Am. Chem. Soc.* **2004**, *126*, 7422–7424.

(12) Lee, C.-C.; Liu, Y.; Reineke, T. M. General structure-activity relationship for poly(glycoamidoamine)s: The effect of amine density on cytotoxicity and DNA delivery efficiency. *Bioconjugate Chem.* **2008**, *19* (2), 428–440.

(13) Liu, Y.; Reineke, T. M. Poly(glycoamidoamine)s for gene delivery. Structural effects on cellular internalization, buffering capacity, and gene expression. *Bioconjugate Chem.* **2007**, *18* (1), 19–30.

(14) McLendon, P. M.; Fichter, K. M.; Reineke, T. M. Poly(glycoamidoamine) Vehicles Promote pDNA Uptake through Multiple Routes and Efficient Gene Expression via Caveolae-Mediated Endocytosis. *Mol. Pharmaceutics* **2010**, *7* (3), 738–750.

(15) Liu, Y.; Reineke, T. M. Degradation of Poly(glycoamidoamine) DNA Delivery Vehicles: Polyamide Hydrolysis at Physiological Conditions Promotes DNA Release. *Biomacromolecules* **2010**, *11* (2), 316–325.

cell-signaling molecules such as growth factors.<sup>16,17</sup> They are also vital to tissue function, forming structural elements that are essential for the function of specialized tissue, such as the compressibility of cartilage, tensile strength of skin and tendons, and the viscoelasticity of blood vessels.<sup>18</sup> Changes in GAG structure have also been implicated in tumorigenesis.<sup>19</sup> GAGs participate in receptor clustering and can aid in binding of extracellular molecules and particles for internalization.<sup>20</sup> GAGs are the most anionic component of the cell membrane, due to post-translational N- and O-sulfation on the sugars.<sup>21</sup> Moreover, GAGs have been demonstrated to be involved in the docking of several viral pathogens, such as human immunodeficiency virus-1,<sup>22</sup> adeno-associated virus,<sup>23</sup> and herpes simplex virus.<sup>21</sup> These findings have led to the speculation of their involvement as a primary receptor for cationic nucleic acid delivery vehicles.

Previous studies suggest that GAGs may serve as a primary receptor to cationic nucleic acid delivery vehicles, and many important studies have been published demonstrating involvement of GAGs in the internalization of polymer-,<sup>16,24–27</sup> lipid-<sup>28–30</sup> and peptide-based<sup>31–36</sup> DNA transport vehicles.

GAGs have also been proposed as a barrier to nonviral DNA delivery systems.<sup>25,26</sup> Many of these studies have suggested that vehicle–GAG interactions occur primarily with cell surface heparan sulfate (HS) proteoglycans.<sup>27,32,37</sup> However, due to the strongly anionic nature of HS, interactions of GAGs with positively charged polyplexes or lipopolyplexes may not necessarily lead to receptor-mediated cell entry.<sup>17</sup> Indeed, many studies have used highly sulfated GAGs, such as heparin, to competitively displace DNA from a vehicle as a measure of the DNA binding strength of the carrier,<sup>9,38–40</sup> but these interactions do not suggest any specific affinity between polymer and heparin. Therefore, an in-depth probe of many different GAGs, specifically GAGs that are presented on mammalian cell surfaces, is warranted.

The present study was designed to examine the interactions of PGAA-containing polyplexes with several different cell surface GAGs. Specifically, we sought identification of particular GAG structures and the contribution of electrostatics that lead to efficient cellular internalization of polyplexes.

- (16) Mislick, K. A.; Baldeschwieler, J. D. Evidence for the role of proteoglycans in cation-mediated gene transfer. *Proc. Natl. Acad. Sci. U.S.A.* **1996**, *93*, 12349–12354.
- (17) Kjell  n, L.; Lindahl, U. Proteoglycans: Structures and Interactions. *Annu. Rev. Biochem.* **1991**, *60*, 443–475.
- (18) Iozzo, R. V. *Proteoglycans: structure, biology, and molecular interactions*; Marcel Dekker, Inc: New York, 2000.
- (19) Yip, G. W.; Smollich, M.; Gotte, M. Therapeutic value of glycosaminoglycans in cancer. *Mol. Cancer Ther.* **2006**, *5* (9), 2139–2148.
- (20) Woods, A.; Oh, E.-S.; Couchman, J. R. Syndecan Proteoglycans and Cell Adhesion. *Matrix Biol.* **1998**, *17*, 477–483.
- (21) Park, P. W.; Reizes, O.; Bernfield, M. Cell surface heparan sulfate proteoglycans: selective regulators of ligand-receptor encounters. *J. Biol. Chem.* **2000**, *275* (39), 29923–29926.
- (22) Zhang, Y. J.; Hatzioannou, T.; Zang, T.; Braaten, D.; Luban, J.; Goff, S. P.; Bieniasz, P. D. Envelope-dependent, cyclophilin-independent effects of glycosaminoglycans on human immunodeficiency virus type 1 attachment and infection. *J. Virol.* **2002**, *76* (12), 6332–6343.
- (23) Summerford, C.; Samulski, R. J. Membrane-Associated Heparan Sulfate Proteoglycan is a Receptor for Adeno-Associated Virus Type 2 Virions. *J. Virol.* **1998**, *72* (2), 1438–1445.
- (24) Hess, G. T.; Humphries IV, W. H.; Fay, N. C.; Payne, C. K. Cellular Binding, Motion, and Internalization of Synthetic Gene Delivery Polymers. *Biochim. Biophys. Acta* **2007**, *1773*, 1583–1588.
- (25) R  ponen, M.; Honkakoski, P.; Tammi, M.; Urtti, A. Cell-surface glycosaminoglycans inhibit cation-mediated gene transfer. *J. Gene Med.* **2004**, *6* (4), 405–414.
- (26) R  ponen, M.; Ronkko, S.; Honkakoski, P.; Pelkonen, J.; Tammi, M.; Urtti, A. Extracellular glycosaminoglycans modify cellular trafficking of lipopolyplexes and polyplexes. *J. Biol. Chem.* **2001**, *276* (36), 33875–33880.
- (27) Kopatz, I.; Remy, J.-S.; Behr, J.-P. A Model for Non-Viral Gene Delivery: Through Syndecan Adhesion Molecules and Powered by Actin. *J. Gene Med.* **2004**, *6*, 769–776.
- (28) Belting, M.; Petersson, P. Protective Role for Proteoglycans Against Cationic Lipid Cytotoxicity Allowing Optimal Transfection Efficiency in vitro. *Biochem. J.* **1999**, *342*, 281–286.
- (29) Mounkes, L. C.; Zhong, W.; Cipres-Palacin, G.; Heath, T. D.; Debs, R. J. Proteoglycans mediate cationic liposome-DNA complex-based gene delivery in vitro and in vivo. *J. Biol. Chem.* **1998**, *273* (40), 26164–26170.
- (30) R  ponen, M.; Yla-Herttuala, S.; Urtti, A. Interactions of polymeric and liposomal gene delivery systems with extracellular glycosaminoglycans: physicochemical and transfection studies. *Biochim. Biophys. Acta* **1999**, *1415* (2), 331–341.
- (31) Fuchs, S. M.; Raines, R. T. Pathway for Polyarginine Entry into Mammalian Cells. *Biochemistry* **2004**, *43*, 2438–2444.
- (32) Nascimento, F. D.; Hayashi, M. A. F.; Kerkis, A.; Oliveira, V.; Oliveira, E. B.; Radis-Baptista, G.; Nader, H. B.; Yamane, T.; Tersariol, I. L. D.; Kerkis, I. Crotamine mediates gene delivery into cells through the binding to heparan sulfate proteoglycans. *J. Biol. Chem.* **2007**, *282* (29), 21349–21360.
- (33) Sandgren, S.; Cheng, F.; Belting, M. Nuclear Targeting of Macromolecular Polyanions by an HIV-Tat Derived Peptide. *J. Biol. Chem.* **2002**, *277* (41), 38877–38883.
- (34) Suzuki, T.; Futaki, S.; Niwa, M.; Tanaka, S.; Ueda, K.; Sugiura, Y. Possible existence of common internalization mechanisms among arginine-rich peptides. *J. Biol. Chem.* **2002**, *277* (4), 2437–2443.
- (35) Kim, H. H.; Lee, W. S.; Yang, J. M.; Shin, S. Basic Peptide System for Efficient Delivery of Foreign Genes. *Biochim. Biophys. Acta* **2003**, *1640*, 129–136.
- (36) Kosuge, M.; Takeuchi, T.; Nakase, I.; Jones, A. T.; Futaki, S. Cellular internalization and distribution of arginine-rich peptides as a function of extracellular peptide concentration, serum, and plasma membrane associated proteoglycans. *Bioconjugate Chem.* **2008**, *19* (3), 656–664.
- (37) Berry, D.; Lynn, D. M.; Sasisekharan, R.; Langer, R. Poly (B-amino ester)s Promote Cellular Uptake of Heparin and Cancer Cell Death. *Chem. Biol.* **2004**, *11*, 487–498.
- (38) Layman, J. M.; Ramirez, S. M.; Green, M. D.; Long, T. E. Influence of Polycation Molecular Weight of Poly(2-dimethyl-aminoethyl methacrylate)-Mediated DNA Delivery in Vitro. *Biomacromolecules* **2009**, *10*, 1244–1252.
- (39) Srinivasachari, S.; Liu, Y.; Prevette, L. E.; Reineke, T. M. Effects of trehalose click polymer length on pDNA complex stability and delivery efficacy. *Biomaterials* **2007**, *28*, 2885–2898.
- (40) Hwang, S. J.; Bellocq, N. C.; Davis, M. E. Effects of Structure of  $\beta$ -Cyclodextrin-Containing Polymers on Gene Delivery. *Bioconjugate Chem.* **2001**, *12* (2), 280–290.



In these studies, we have chosen to study heparan sulfate (HS), two forms of chondroitin sulfate (CSA and CSC), dermatan sulfate (DS), and hyaluronate (HA) due to their existence in mammalian tissues, and on HeLa cells, our model cell line.<sup>41,42</sup> We have studied the effect of competitive uptake inhibition with free GAG, as well as the effect of GAG removal and removal of sulfate groups on cellular internalization. We have also developed and applied a series of biophysical techniques to investigate the nature of the polyplex–GAG interaction and structural changes to the polyplex that may occur upon interaction with the cell surface. We report evidence that PGAA-containing polyplexes interact with GAGs in a manner that facilitates their uptake into mammalian cells. The affinity of GAGs for these polyplexes is not solely governed by electrostatics, and the presence of sulfated GAGs leads to efficient cellular uptake. Certain polyplexes appear to prefer binding to particular GAGs, suggesting that other interactions may occur between the carbohydrates in the polymer and the GAG chains; this may present a strategy to improve cell specificity. Upon interaction with GAGs, the polyplex becomes surrounded by GAGs such that the surface charge becomes negative and the polyplex structure begins to decompact without dissociating. To the best of our knowledge, this study is the most in-depth probe into polyplex–GAG interactions, and it provides a more detailed understanding of polyplex binding to the cell surface.

## Experimental Section

**Chemical and Biological Reagents.** All chemical reagents were purchased from Sigma-Aldrich (St. Louis, MO) unless noted otherwise. All four poly(glycoamidoamine)s (PGAAs)—[poly(galactaramidopentaethylenetetramine) (G4), poly(D-glucaramidopentaethylenetetramine) (D4), poly(D-mannaramidopentaethylenetetramine) (M4), and poly(L-tartaramidopentaethylenetetramine) (T4)]—were synthesized and purified as previously described.<sup>9–11</sup> Plasmid DNA (pDNA) pCMV $\beta$  was purchased from Aldevron (Fargo, ND). pCMV $\beta$  was labeled with Cy5 using a Label *IT* kit (Mirus, Madison, WI) at 1/10 the labeling ratio suggested by the manufacturer and purified using QIAquick PCR purification kit (Qiagen, Valencia, CA). Jet-PEI solution was purchased from Avanti Polar Lipids (Birmingham, AL). Propidium iodide (PI) and dimethyl sulfoxide were purchased from Molecular Probes (Eugene, OR). Chondroitin sulfate A was purchased from Calbiochem (Darmstadt, Germany). Unless otherwise noted, all dilutions, including N/P dilutions of the PGAAs and

pDNA, were made in DNase/RNase-free H<sub>2</sub>O (Gibco, Carlsbad, CA).

**Polyplex Preparation.** PGAA–DNA polyplexes were formulated at an N/P ratio of 20 for all experiments. Jet-PEI polyplexes were formed at an N/P ratio of 5. Polyplexes were formed with Cy5-pCMV $\beta$ . The DNA concentration used for polyplex formulations was 0.02 mg/mL (prior to polymer addition), and an equal volume of polymer solution at the appropriate N/P ratio was added to the DNA solution and incubated at room temperature for at least 30 min. For PGAA polymers, N/P ratios were calculated using only the secondary amine nitrogens. Uncomplexed DNA control (DNA only) was prepared using nuclease-free water in place of the polymer solution.

**Cell Culture.** All cell culture products, unless otherwise noted, were purchased from Gibco/Invitrogen (Carlsbad, CA). HeLa (human adenocervical carcinoma) cells and wild-type and mutant (pgsA-745 and pgsD-677, respectively) CHO (Chinese hamster ovary) cells were purchased from ATCC (Manassas, VA). All cell lines were subcultured once per week. HeLa cells were grown in advanced Dulbecco's modified Eagle's medium (DMEM) supplemented with 2% heat-inactivated fetal bovine serum (FBS), 1% L-glutamine, and 1% antibiotic/antimycotic (Ab/Am). CHO cells were grown in F-12K medium (ATCC) supplemented with 10% FBS and 1% Ab/Am. CHO cells were seeded for transfection in the same medium, and HeLa cells were seeded for transfections in DMEM containing GlutaMAX and supplemented with 10% FBS, and 1% Ab/Am. Cells were determined to be free of mycoplasma contamination using MycoAlert mycoplasma detection kit (Lonza, Rockland, ME). Unless otherwise noted, all incubations of cells in flasks or plates were performed at 37 °C and 5% CO<sub>2</sub>.

**Effect of Competitive Inhibition on Polyplex Uptake by GAGs.** Experiments were done similarly to work by Mislick and Baldeschwieler.<sup>16</sup> Briefly, HeLa cells were seeded at  $1.5 \times 10^5$  cells/well in DMEM containing 10% FBS in 6-well tissue culture plates (Corning; Corning, NY) 24 h prior to treatment. After removing medium and washing cells with PBS, 600  $\mu$ L of 60  $\mu$ g/mL GAG in OptiMEM reduced-serum medium was added to each well and incubated for 15 min at 4 °C. Polyplexes (300  $\mu$ L) were added to each well and incubated for 2 h, then 3 mL of DMEM was added and cells were incubated for 30 min. Cells were detached with 500  $\mu$ L of trypsin–EDTA, quenched with DMEM (1 mL), and the contents of each well were collected into Falcon Tubes (BD Biosciences, San Jose, CA). Cells were centrifuged at 4 °C and 1250 rpm for 10 min. The cell pellets were rinsed with PBS and centrifuged again at identical conditions. The supernatants were removed, and the cell pellets were suspended in PBS containing 2% FBS. Cellular uptake of Cy5-pCMV $\beta$  was measured on a FACS Calibur flow cytometer (BD Biosciences, San Jose, CA). Cy5 was excited using a 633 nm helium–neon (HeNe) laser and detected using a 667/20 nm band-pass filter. Appropriate gating was performed using untransfected cells to ensure that autofluo-

(41) Charnaux, N.; Brule, S.; Chaigneau, T.; Saffar, L.; Sutton, A.; Hamon, M.; Prost, C.; Lievre, N.; Vita, C.; Gattegno, L. RANTES (CCL5) induces a CCR5-dependent accelerated shedding of syndecan-1 (CD138) and syndecan-4 from HeLa cells and forms complexes with the shed ectodomains of these proteoglycans as well as those of CD44. *Glycobiology* **2005**, *15* (2), 119–130.

(42) Matsuno, Y.; Kinoshita, M.; Kakehi, K. Electrophoretic analysis of di- and oligosaccharides derived from glycosaminoglycans on microchip format. *J. Pharm. Biomed. Anal.* **2004**, *36*, 9–15.

rescence was not measured as cellular uptake; 10,000–20,000 gated events were collected for each sample.

**Chlorate Desulfation.** Experimental details were based upon previously published work.<sup>16,43</sup> For cellular uptake analysis, HeLa cells were seeded at  $6 \times 10^4$  cells/well in 6-well plates and incubated for 16 h prior to treatment. After 16 h, medium was replaced with 3 mL of sulfate-free DMEM containing 35 mM sodium chlorate. Cells were incubated in this medium for an additional 28 h. Polyplexes (300  $\mu$ L) were diluted with OptiMEM (600  $\mu$ L), added to each well and incubated for 4 h, then 3 mL of sulfate-free DMEM was added and the cells were incubated for 30 min. Cells were rinsed with heparin (Sigma, 2 mg/mL in PBS, ammonium salt from porcine intestinal mucosa), detached with trypsin–EDTA, quenched with DMEM (1 mL), and the contents of each well were collected into Falcon Tubes (BD Biosciences). Cells were centrifuged at 4 °C and 1250 rpm for 10 min. The supernatants were removed, and the cell pellets were rinsed with PBS and centrifuged again at identical conditions before resuspending in PBS containing 2% FBS. Cellular uptake of Cy5-pCMV $\beta$  was measured on a FACS Calibur flow cytometer. Cy5 was excited using a 633 nm HeNe laser and detected using a 667/20 nm band-pass filter. Replicate experiments were analyzed using a FACS Canto II flow cytometer (BD Biosciences), and Cy5 was excited using a 633 nm HeNe laser and detected with a 660/20 nm band-pass filter. Appropriate gating was performed using untransfected cells to ensure that autofluorescence was not measured as cellular uptake; 10,000–20,000 gated events were collected for each sample. Results presented are averages of four experiments.

**Comparative Internalization of GAG-Containing and GAG-Deficient Cells.** Experiments were done similarly to work by Mislick and Baldeschwieler.<sup>16</sup> For cellular uptake analysis, CHO and pgsA-745 or pgsD-677 cells were seeded at  $1.5 \times 10^5$  cells/well in 6-well plates and incubated for 24 h prior to treatment. OptiMEM (2 mL) was added to each well, and polyplexes (300  $\mu$ L) were added and incubated for 2 h. F-12K medium (3 mL) was added to each well, and cells were incubated for an additional 30 min. Cells were detached with trypsin–EDTA, quenched with DMEM containing 10% FBS (1 mL), and the contents of each well were collected into Falcon Tubes (BD Biosciences). Cells were centrifuged at 4 °C and 1250 rpm for 10 min. The supernatants were removed, and then the cell pellets were rinsed with PBS and centrifuged again at identical conditions. The supernatant was removed, and the cell pellets were resuspended in PBS containing 2% FBS. Cellular uptake of Cy5-pCMV $\beta$  was measured on a FACS Canto II flow cytometer (BD Biosciences). Propidium iodide (PI, 5  $\mu$ g/mL) was added to each tube and gently vortexed 2–5 min prior to analysis. Appropriate gating was performed using untransfected cells to ensure that autofluorescence and dead

cells (PI-positive) were excluded from subsequent analysis. Cy5 was excited using a 633 nm HeNe laser and detected with a 660/20 nm band-pass filter; PI was excited with a 488 nm solid-state laser, and fluorescence emission was detected by a 670 nm long-pass filter. A total of 10,000–20,000 gated events were collected for each sample. Results presented are averages of at least two replications.

**Gel Dissociation Assay.** Polyplexes were prepared at N/P of 20, using pCMV $\beta$  at a final concentration of 0.1 mg/mL, by adding 10  $\mu$ L of polymer into 10  $\mu$ L of DNA. Polyplexes were incubated at room temperature for 30 min. The GAG solution in water (10  $\mu$ L) was added to the polyplex solution, and the resulting mixture was incubated for 15 min. BlueJuice loading buffer (3  $\mu$ L, Invitrogen) was added to each tube, and an aliquot (10  $\mu$ L) of the resulting solution was added to the appropriate well of a 0.6% agarose gel containing 60  $\mu$ g of ethidium bromide (Molecular Probes). Samples were electrophoresed for 40–60 min at 65 V. The concentration of GAG-induced dissociation was estimated by the first evidence of DNA migration in the lane of the gel.

**Effect of GAG on Polyplex Size and Surface Charge.** Polyplexes were prepared as described earlier, and GAG stock solutions were diluted to 60  $\mu$ g/mL. Polyplexes (300  $\mu$ L) were mixed with 600  $\mu$ L of H<sub>2</sub>O (for the control) or appropriate GAG solution and then incubated for 60 min. Particle size and  $\zeta$ -potential were measured at 25 °C using a ZetaSizer NanoSeries ZS dynamic light scattering instrument (Malvern; Worcestershire, U.K.), equipped with a 4 mW HeNe (633 nm) laser with 173° scattering angle.  $\zeta$ -Potential measurements were measured with laser Doppler velocimetry at a 17° scattering angle. The free GAGs in solution did not form spherical structures, as evidenced by our inability to detect them by DLS (data not shown). Therefore, any changes to polyplex size or surface chemistry should be the result of GAG accumulation on the surface, rather than interference of the measurements by GAGs.

**Fluorescence Assay for GAG-Induced Alterations in Polyplex Structure.** PicoGreen (Molecular Probes) was diluted at a 1:200 ratio in H<sub>2</sub>O, and the resulting solution was used to dilute DNA (pCMV $\beta$ ) to 0.02 mg/mL. The DNA solution (25  $\mu$ L) was added to wells of black 96-well fluorescence microplates, and 25  $\mu$ L of G4 polymer solution or H<sub>2</sub>O (for controls) was added to each well. Plates were gently rocked for 5 min and allowed to rest 30 min for complex formation. GAG stocks in H<sub>2</sub>O were diluted to concentrations of 10–90  $\mu$ g/mL, and 50  $\mu$ L portions of the above solutions (or H<sub>2</sub>O for controls) were added to appropriate wells, such that each polymer was incubated with each GAG at the above concentration range. Plates were placed on a shaker and gently rocked for 30 min. Fluorescence was measured after 2 h using the GENios Pro plate reader (Tecan, Research Triangle Park, NC);  $\lambda_{\text{ex}}$  = 488 nm,  $\lambda_{\text{em}}$  = 535/20 nm band-pass filter. The increase in fluorescence as a result of GAG incubation is normalized against controls of uncomplexed DNA (fluorescence maximum,

(43) Baeuerle, P. A.; Huttner, W. B. Chlorate - A Potent Inhibitor of Protein Sulfation in Intact Cells. *Biochem. Biophys. Res. Commun.* **1986**, *141* (2), 870–877.

normalized to 1) and fluorescence from wells containing polyplexes but not GAGs (fluorescence minimum, normalized to 0).

**Visualizing Polyplex-GAG Interactions with Transmission Electron Microscopy.** Polyplexes were prepared as described above, and 25  $\mu\text{L}$  portions of GAGs (heparin, HS, CSA, CSC, DS, HA; 60  $\mu\text{g}/\text{mL}$ ) were added to polyplexes (50  $\mu\text{L}$ ) and incubated for 15 min. Polymer-pDNA-GAG complexes (5  $\mu\text{L}$ ) were applied to a 400-mesh copper-on-carbon grid (Electron Microscopy Sciences, Hatfield, PA) and incubated 1 min before wicking away the solution. Uranyl acetate stain (5  $\mu\text{L}$ , 2% w/v) was applied to the grid and then wicked away. Polyplexes were imaged using a Philips EM420 transmission electron microscope.

**Measuring Polyplex:GAG Binding Affinity with QCM.** GAGs (40  $\mu\text{g}/\text{mL}$ ) and polyplexes were prepared as described above. Consistency in polyplex formation was verified through particle size and zeta potential measurements. Polyplex-GAG binding was measured with gold coated sensors using quartz crystal microbalance (QCM) on a Q-Sense E4 QCM (Q-sense; Vastra Frolunda, Sweden). The sensors were precleaned prior to each experiment via UV/ozone irradiation, and rinsed with a 5:1:1 mixture of pure water, 25% ammonia, and 30% hydrogen peroxide, respectively, at 75  $^{\circ}\text{C}$  for 5 min before thorough rinsing with pure water, drying under nitrogen, and further UV/ozone irradiation. Clean gold sensors were equilibrated in air, followed by pure water equilibration. Polyplex solution was applied across the sensor at a rate of 0.2 mL/min. Upon stabilization of frequency measurements, pure water was run across the sensor to ensure that polyplexes were irreversibly bound. GAG solution was introduced at the same rate as above, until frequency stabilization was attained. A pure water rinse was used to remove irreversibly bound GAGs. Relative GAG binding affinity to G4 polyplexes was assessed through the measured change in frequency (after pure water rinse to remove irreversibly bound polyplexes and GAGs), which is directly related to increase in mass due to GAG binding. Frequency shifts of the fifth harmonic were used to calculate the mass increase to the crystal upon GAG binding, using the Sauerbrey equation ( $c = 17.7 \text{ ng cm}^{-2} \text{ Hz}^{-1}$ , and is specific for the crystal):

$$\Delta m = \Delta f c$$

Presented data is an average of two independent experiments.

## Results

For all *in vitro* experiments contained herein, cellular internalization is measured by flow cytometry. Polyplexes are fluorescently tagged using pDNA that has been conjugated to Cy5. Cellular internalization is determined by an increase in intracellular fluorescence intensity with respect to untransfected cells, and the percent change in internalization is assessed through comparison to a control in which cells were transfected with polyplex but without GAG inhibition. The cell purification protocol outlined in the

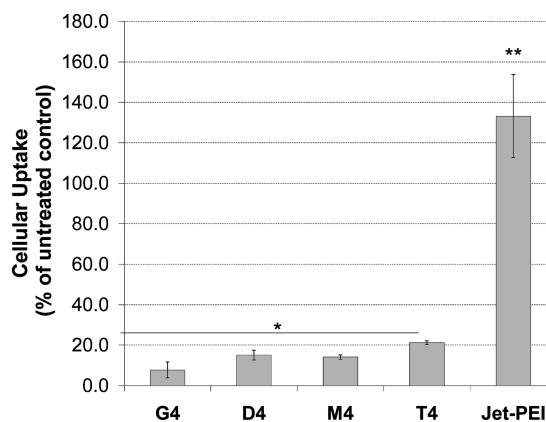


**Figure 2.** Effect of GAG desulfation on PGAA and PEI polyplex internalization. HeLa cells were incubated with sodium chlorate (35 mM) for 36 h prior to transfection with PGAA or PEI polyplexes formulated with Cy5-labeled pDNA. Intracellular fluorescence was measured by flow cytometry. Data is presented as the percent of internalization, measured by intracellular Cy5 fluorescence intensity, with respect to control cells treated with polyplex but without chlorate. GAG desulfation caused strong (~80% or greater) reduction in intracellular fluorescence for all four PGAAAs, whereas PEI polyplexes yielded slightly greater intracellular fluorescence after GAG desulfation. \* $p < 0.05$ . Jet-PEI (\*\*) is statistically different from the PGAAAs ( $p < 0.0001$ ).

Experimental Section was sufficient to remove all polyplexes bound to the cell surface, as heparin washing<sup>44</sup> had no effect on Cy5-associated cell fluorescence (data not shown). Therefore, reported fluorescence is a result of intracellular complexes.

The requirement of sulfated GAGs for internalization was explored by desulfating the GAGs using sodium chlorate. Chlorate inhibits PAPS synthetase, a sulfotransferase enzyme which conjugates the amine and hydroxyl groups within the GAG chains with sulfate groups.<sup>43</sup> Chlorate has been shown to inhibit PG sulfation by as much as 90–95%.<sup>43,45</sup> The resultant cell-surface GAGs exist in their nonsulfated form, dramatically reducing the charge of the GAGs. When we used chlorate to inhibit GAG sulfation (Figure 2), a decrease in cellular uptake of at least 80% was observed for the PGAA polyplexes, suggesting that the highly charged nature of the GAGs is necessary to bring the polyplexes into contact with the cell. We used linear polyethylenimine (PEI), a well-studied polymeric vehicle for nucleic acid delivery, for comparison with the PGAAAs. Upon desulfation of GAGs on HeLa cells, a modest increase in internalization was observed (as noted by a negative percent decrease in internalization

- (44) von Gersdorff, K.; Sanders, N. N.; Vandenbroucke, R.; De Smedt, S. C.; Wagner, E.; Ogris, M. The Internalization Route Resulting in Successful Gene Expression Depends on both Cell Line and Polyethylenimine Polyplex Type. *Mol. Ther.* **2006**, *14* (5), 745–753.
- (45) Humphries, D. E.; Silbert, J. E. Chlorate: A Reversible Inhibitor of Proteoglycan Sulfation. *Biochem. Biophys. Res. Commun.* **1988**, *154* (1), 365–371.



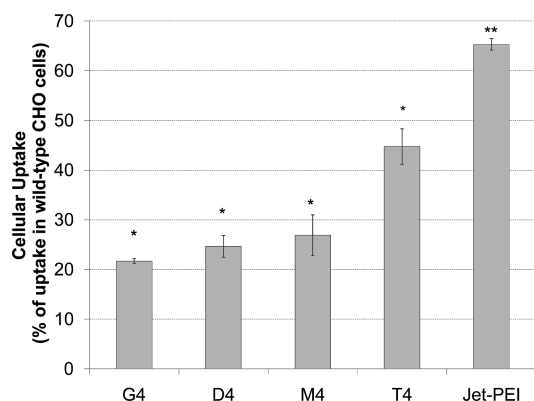


**Figure 3.** Comparison of PGAA and PEI polyplex internalization in GAG-containing vs GAG-lacking cells. CHO (wild type, GAG-containing) and pgsA-745 (mutant, GAG-lacking) cells were transfected with PGAA or PEI polyplexes containing Cy5-labeled pDNA. Presented data is intracellular Cy5 fluorescence intensity, measured by flow cytometry. Controls include untreated cells and cells transfected with Cy5-labeled DNA alone. Intracellular fluorescence was significantly ( $\sim 75\%$ ) reduced in GAG-lacking cells for G4, D4, and M4, more modestly ( $\sim 55\%$ ) reduced for T4, and minimally (35%) reduced for PEI polyplexes.  $*p = 0.0001$ ;  $**p = 0.005$ .

in Figure 2). These results suggest that the PGAA polyplexes likely trigger internalization through GAG interaction, however, an alternate route of cellular internalization is possibly used by PEI polyplexes.

GAG involvement in cellular uptake was studied further by examining how polyplex internalization is affected by absence of cell-surface GAGs. Wild-type Chinese hamster ovary (CHO) cells and a non-GAG-expressing variant, pgsA-745, were used for this study. The mutant cells lack xylosyltransferase, an enzyme responsible for linking a xylose residue onto the core protein of proteoglycans,<sup>16</sup> which serves as a primer for GAG synthesis. Wild-type CHO cells contain GAGs on their surface, so the cellular internalization profiles between the two cell lines can be compared to observe the importance of GAGs in internalization. Upon removal of GAGs (Figure 3), a large decrease ( $\sim 75\%$ ) in cellular internalization for polyplexes formed with three PGAA—G4, D4, and M4—was observed, suggesting the necessity of cell-surface GAGs for efficient uptake of these polyplexes. Only 55% inhibition was seen for T4 polyplexes (contains two hydroxyls in the repeat unit), suggesting that they can internalize through a GAG-independent method more efficiently than the other PGAA—G4, D4, and M4—polyplexes studied, which contain four hydroxyl groups in the polymer repeat unit. Similar to the previous data, the internalization of PEI polyplexes was inhibited to a much lower degree in the absence of GAGs.

A similar experiment was completed using another CHO mutant cell line, pgsD-677. This cell line is deficient in *N*-acetylglucosaminyltransferase and glucuronyltransferase and is deficient in heparan sulfate (HS) biosynthesis, while

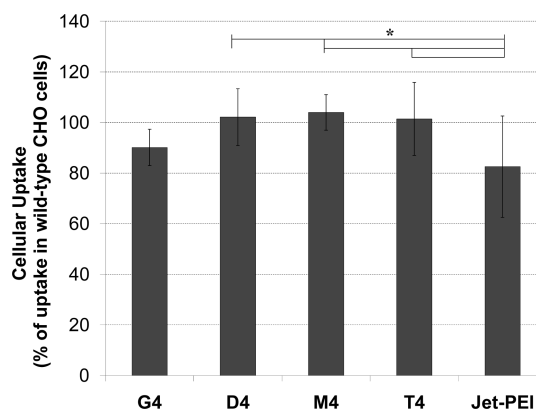


**Figure 4.** Comparison of PGAA and PEI polyplex internalization in HS-containing vs HS-lacking cells. CHO (wild type, HS-containing) and pgsD-677 (mutant, HS-deficient) cells were transfected with PGAA or PEI polyplexes containing Cy5-labeled pDNA. Data is presented as the percent of internalization into pgsD-677 mutants lacking HS, measured by intracellular Cy5 fluorescence intensity, with respect to the wild type CHO cells. Intracellular fluorescence was decreased to a small degree in HS-lacking cells for PGAA and PEI polyplexes.  $*p < 0.005$ ,  $**p < 0.001$ .

still producing chondroitin sulfate proteoglycans.<sup>46</sup> These cells allow us to assess the internalization of PGAA polyplexes in the absence of only heparan sulfate. The results of the cellular internalization experiments (as assessed by flow cytometry) are presented in Figure 4. PGAA polyplex uptake is not significantly inhibited in the absence of HS. This suggests that, while PGAA appears to have affinity for HS, this particular GAG is not necessary for internalization. Other GAGs, including chondroitin (CS) and dermatan sulfate (DS), are still available for polyplex binding, and internalization may occur through PGAA–CS/PGAA–DS interactions, rather than PGAA–HS interactions. These results suggest that polyplex binding to the cell surface is not mediated solely by charge (Figure S1 in the Supporting Information, charge density of GAGs: heparin > HS > DS > CSC = CSA > HA).

PGAA polyplexes appear to enter the cell mostly through interactions with sulfated GAGs, and understanding these interactions is important to elucidating how endocytosis is triggered. Specifically, we are interested in identifying differences in the affinities between each PGAA polyplex type and individual GAGs. In a preliminary experiment to examine these interactions, solutions of free GAGs (40  $\mu\text{g}/\text{mL}$ ) were used to competitively inhibit uptake of polyplexes into HeLa cells (Figure S2 in the Supporting Information). A decrease in uptake would suggest that polyplexes bind to GAGs in the medium, causing less binding to occur at the

(46) Lidholt, K.; Weinke, J. L.; Kiser, C. S.; Lugemwa, F. N.; Bame, K. J.; Cheifetz, S.; Massagué, J.; Lindahl, U.; Esko, J. D. A single mutation affects both *N*-acetylglucosaminyltransferase and glucuronyltransferase activities in a Chinese hamster ovary cell mutant defective in heparan sulfate biosynthesis. *Proc. Natl. Acad. Sci. U.S.A.* **1992**, 89 (6), 2267–2271.

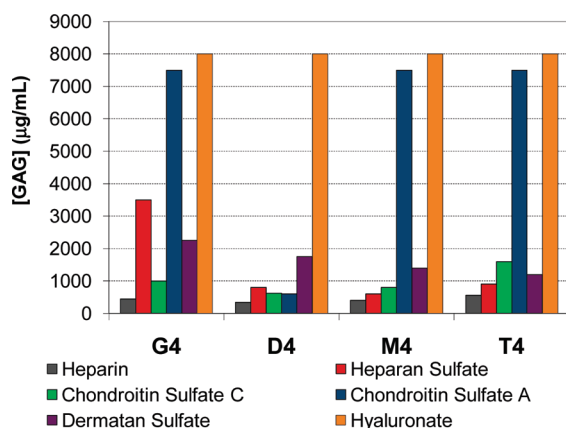


**Figure 5.** Dissociation of PGAA polyplexes by GAGs. PGAA polyplexes were incubated with various concentrations of each of five GAGs prior to agarose gel electrophoresis. The plotted values represent the concentrations of GAG (in  $\mu\text{g/mL}$ ) required for the initiation of polyplex dissociation, i.e., the first evidence of DNA migration in the gel. Heparin was the most potent GAG, dissociating all PGAA polyplexes at a lower concentration than the other GAGs. For polyplexes made with G4, M4, and T4, but not D4, CSA was the weakest GAG with respect to polyplex dissociation by a large margin.

cell surface. A large decrease in uptake ( $>60\%$ ) was observed when uptake was inhibited by heparan sulfate, and slightly less inhibition was observed in the presence of chondroitin sulfate C (27%–38%). However, the trend of inhibition does not match the trend of GAG charge (Figure S1 in the Supporting Information), again suggesting a charge-independent affinity between each polyplex type and GAG.

To further investigate the effect of electrostatic interactions, polyplexes were formed and incubated with increasing GAG concentrations. Using agarose gel electrophoresis, we determined the concentration of each GAG type required to completely disassemble the polyplexes (dissociate the PGAA polymers from pDNA). This information can provide insight into any preferential interactions between GAGs and PGAs. The results of these experiments are presented as a tabulated summary (Figure 5) of the GAG concentrations required to dissociate DNA from the four PGAA polyplexes. GAG-induced polyplex disassembly followed an interesting trend:  $\text{Hep} > \text{CSC} > \text{DS} > \text{HS} > \text{CSA}$  (where Hep caused polyplex disassembly at the lowest GAG concentrations (most dissociative GAG) and CSA caused polyplex disassembly at the highest GAG concentration (least dissociative GAG)). Heparin, the most highly sulfated GAG, induced release of DNA at lower concentrations than the other GAGs. This finding is expected due to the high charge-density of heparin. However, heparin is produced by mast cells<sup>47</sup> and is cleaved from its core protein;<sup>48</sup> heparin should not be present on the surfaces of HeLa cells. The trend of dissociation observed

for G4, D4, and M4 does not correspond with increasing GAG negative charge, suggesting interactions other than electrostatics mediate the affinity between the GAG and polyplex. In contrast, the dissociative trend of T4 more closely mimics the trend of increasing GAG negative charge; an exception can be found when examining the dissociation of T4 by chondroitin sulfate, however. CSC and CSA are isoelectronic (Figure S1 in the Supporting Information), but while CSC released DNA from the T4 polyplex at around  $1500 \mu\text{g/mL}$ , CSA did not dissociate the polyplex even at a high concentration of  $7500 \mu\text{g/mL}$ . Similar results were observed with the other polyplex types. Polyplexes formed with G4 and M4 were also unaffected by CSA at a concentration of  $7500 \mu\text{g/mL}$ ; however, D4 polyplexes began to dissociate in the presence of only  $750 \mu\text{g/mL}$  CSA. This suggests that D4 polymer may exhibit preferential affinity for CSA that does not exist with G4, M4 and T4, a feature that could be exploited for cell-type specific targeting. D4 is also dissociated at a lower concentration of CSC than the other PGAs, possibly suggesting a general preference of D4 for chondroitin sulfate. It should also be noted that HA did not dissociate any of the PGAA polyplexes up to a concentration of  $8000 \mu\text{g/mL}$ , which was the highest concentration tested.

Dynamic light scattering was used to observe alterations in polyplex size and surface charge when interacting with GAGs. This study was completed to aid our understanding of the nature of the interaction that occurs between the polyplexes and GAGs. PGAA polyplexes were incubated with a  $40 \mu\text{g/mL}$  aqueous solution of each GAG, and the particle size and  $\zeta$ -potential results of these experiments are shown (Figure 6). As mentioned earlier, free GAGs in solution are not detected by DLS, so these results imply GAG interaction with the polyplex rather than interference with the measurements. A slight reduction in polyplex size, suggestive of GAG-induced polyplex compaction, was observed with most of the GAGs for polyplexes formed with G4 and M4. However, the polyplex size remained mostly unchanged for D4 polyplexes, and the size appeared to increase slightly when T4 polyplexes were incubated with most of the GAGs. Importantly, no GAG elicited a sufficient change in size for any PGAA polyplexes such that internalization would be expected to be impeded, as polyplex size remained in the range of 80–140 nm in all cases. However, when the change in polyplex  $\zeta$ -potential was compared, incubation with GAGs did induce a notable change in surface charge for all PGAA polyplexes. In water, the PGAA polyplexes formed at an N/P ratio of 20 have a positive surface charge (typically +10 to +20 mV), due to protonation of the secondary amines in the polymer backbone at physiological pH. The addition of each GAG into the polyplex solution caused a net negative charge on the polyplex surface. The negative surface charge suggests that the GAG chains accumulate on the surface of the polyplex, forming ternary complexes that are likely due, at least in part, to electrostatic interactions between the polymer amines and the GAG sulfate groups.

(47) Hook, M.; Kjellen, L.; Johansson, S.; Robinson, J. Cell-Surface Glycosaminoglycans. *Annu. Rev. Biochem.* **1984**, *53*, 847–869.

(48) Rabenstein, D. L. Heparin and Heparan Sulfate: Structure and Function. *Nat. Prod. Rep.* **2002**, *19*, 312–331.



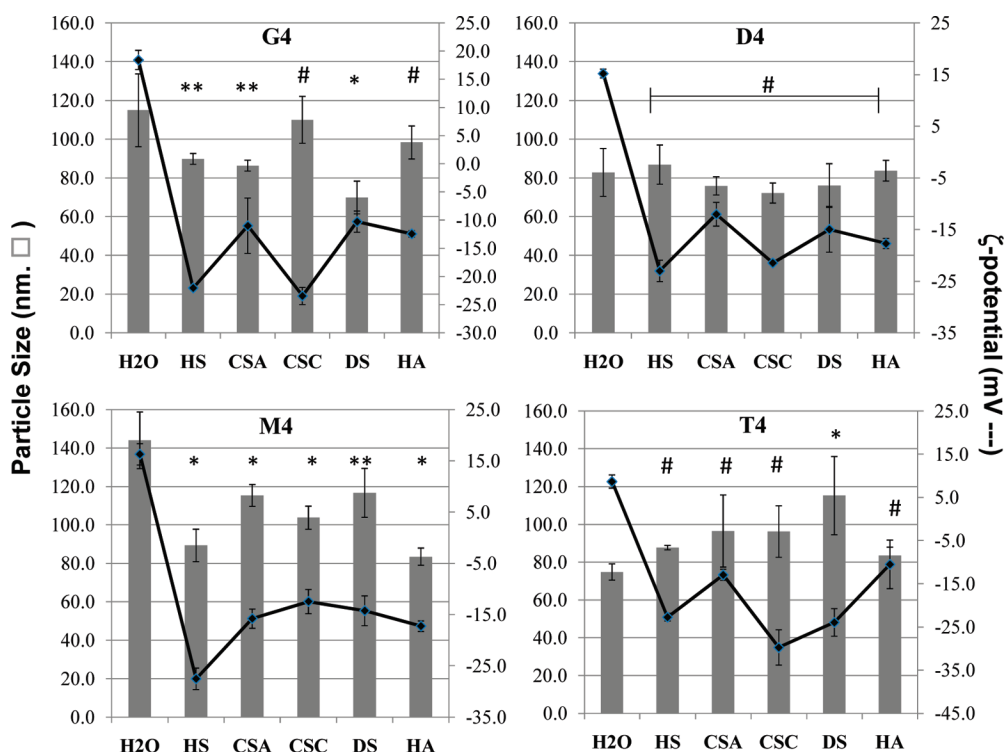


**Figure 6.** Effect of GAG incubation on PGAA polyplex size and surface charge. Each of five GAGs (40  $\mu\text{g}/\text{mL}$  each) or water (control) was incubated with PGAA polyplexes, and the size and  $\zeta$ -potential were measured. Particle size (gray bars) is plotted on the primary (left) axis, and  $\zeta$ -potential (black lines) is plotted on the secondary (right) axis. The sizes of PGAA polyplexes were somewhat affected by various GAGs but stayed within a comparable range to their starting sizes ( $\sim 80$ – $140$  nm). Polyplexes made with each of the four PGAAs exhibited a positive surface charge in water but a negative charge after incubation with each of the five GAGs.  $*p < 0.005$ ;  $**p < 0.05$ ; # not statistically significant from polyplexes in  $\text{H}_2\text{O}$ . Zeta potentials of polyplex with GAG were all statistically different from polyplexes in water.

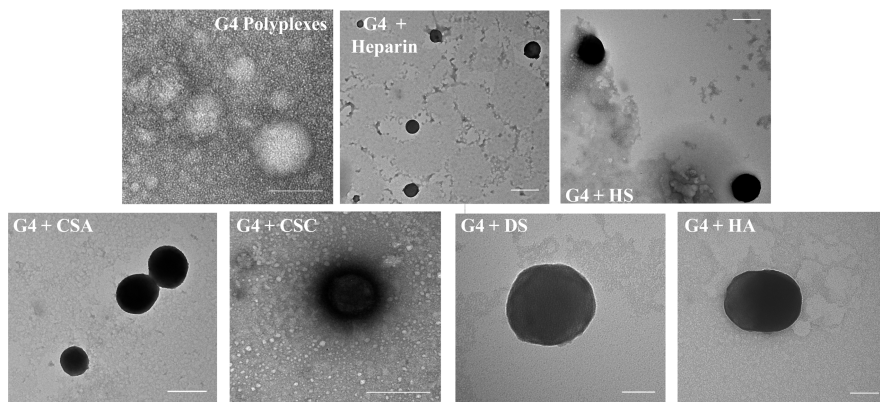


**Figure 7.** Effect of GAG incubation on G4 polyplex appearance via transmission electron microscopy. G4 polyplexes were stained with uranyl acetate. G4 polyplexes in  $\text{H}_2\text{O}$  show a negative staining pattern, due to repulsion of uranyl acetate, where polyplexes incubated with each of the six GAGs show a positive staining pattern, due to the negatively charged polyplexes attracting the cationic stain. Scale bars = 100 nm.

The preceding studies suggest that polyplex internalization may be a result of favorable interactions with GAGs. Polyplexes formed with the PGAA G4 have been shown to elicit high biological activity in a number of cell types, and the following biophysical studies have been completed with this vehicle to better characterize the nature of G4–GAG interactions. Transmission electron microscopy (TEM) was used to visualize the polymer–pDNA–GAG ternary com-

plexes to ensure that the polyplexes remain intact upon interaction with GAGs at the low concentrations used for the DLS experiments. The polyplexes were visualized using TEM (Figure 7), using the PGAA G4 as a representative sample. Polyplexes were visualized by uranyl acetate staining. G4 polyplexes in water are spherical and negatively stained by uranyl acetate, due to charge repulsion between the positively charged polyplex and the cationic stain,

allowing the visualization of polyplexes due to contrast. However, when G4 polyplexes are incubated with GAGs, uranyl acetate accumulates on the polyplex surface due to attraction to the negatively charged polyplex; this was observed for all six GAGs examined. It is to be noted that the polyplexes appear to maintain their spherical morphology in these samples. This confirms the accumulation of GAGs on the surface of polyplexes to form ternary complexes, and provides clues to the nature of interaction at the cell surface.

The PGAA polyplex likely comes into contact with the GAGs in the extracellular matrix prior to internalization, and this interaction may stimulate the cell to initiate endocytosis. The polyplex should stay intact (not be dissociated) when in contact with the GAGs in order to be internalized. For this reason, it is necessary to study the possible structural changes that may occur to the polyplex upon GAG binding. This was investigated using a DNA intercalating dye, PicoGreen (dye fluorescence significantly increases upon DNA intercalation). The fluorescence of this dye decreases upon polyplex formation (relative to DNA alone), likely due to close association of the polymer with the DNA backbone which reduces dye intercalation.<sup>49</sup> This assay was used here to monitor the polyplex disassembly via reincorporation of dye into the pDNA upon GAG–polymer binding. Minimum and maximum fluorescence values were defined, corresponding to intact polyplexes and uncomplexed DNA, respectively, to quantify the amount of fluorescence recovery from PicoGreen intercalating into the accessible pDNA. In this assay, an increase in fluorescence can be directly correlated to decompaction or relaxation of the polyplex, which allows dye molecules to permeate the polyplex and intercalate into accessible pDNA.

Polyplex relaxation was studied with polyplexes formed with one of the PGAA polymers, G4. For these experiments, a GAG concentration range of 0–45  $\mu\text{g/mL}$  was used, as we have shown the polyplexes not to dissociate in this concentration range. It is to be noted that this concentration is still much higher than the GAG concentration the polyplex is likely to encounter on the cell surface.<sup>25</sup> Figure S3 (Supporting Information) shows the results of this experiment. At the lower end of the GAG concentration range examined, as the GAG concentration increases, the fluorescence increases accordingly. These results suggest that more PicoGreen has intercalated into pDNA, which is accessible to dye intercalation due to relaxation of the polyplex structure. This fluorescence increase begins to plateau at a GAG concentration of about 25  $\mu\text{g/mL}$ , suggesting that the polyplex and GAG have reached a stable ternary complex. For polyplexes formed with G4, the fluorescence increases most rapidly with HS, and HS–G4–DNA complexes maintain higher fluorescence levels, with respect to the other GAGs, after the complex stabilizes. By contrast, CSA is the GAG which requires the highest concentration to reach a

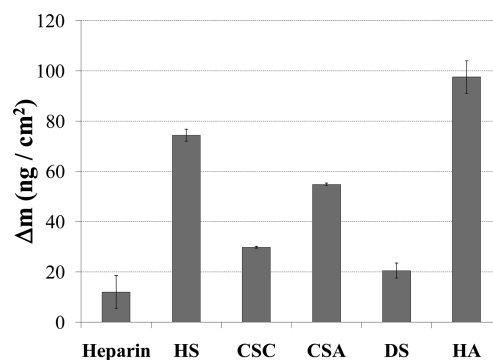


**Figure 8.** Relative binding affinity of GAGs to G4 polyplexes, as measured by QCM. Data is represented as a change in crystal mass upon GAG binding. Positive numbers indicate a mass increase correlated to GAG binding to polyplex monolayer. Highest relative binding affinity to G4 polyplexes was observed with HA, followed by HS, CSA, and CSC. DS and heparin have the lowest binding to G4.

stable complex with G4 polyplexes. CSA induces G4 polyplex decompaction such that nearly 50% of the relative fluorescence is restored, suggesting that G4 polyplexes in contact with CSA may have the most highly relaxed structure. As expected, HA, the least-charged GAG, shows the least fluorescence recovery, suggesting less polyplex relaxation. The relative order of polyplex “loosening” via this method followed a general trend: HS  $\geq$  CSA  $\geq$  CSC  $\geq$  DS  $\geq$  HA (HS causes higher polyplex relaxation, and HA causes the lowest).

The preceding experiments provide valuable clues to the nature of polyplex–GAG interactions that occur at the cell surface and facilitate polyplex internalization. However, many of these studies are indirect measures of polyplex affinity for individual GAGs. Relative polyplex–GAG affinity was directly measured using quartz crystal microbalance (QCM). In this technique, a dilute GAG solution (40  $\mu\text{g/mL}$ ) is flowed across a polyplex monolayer bound to a gold-coated quartz crystal. GAG binding to the polyplex will cause a measurable increase in crystal mass, which can be related to G4 affinity to the GAG. These experiments were completed with each of the aforementioned GAGs. Representative experiments and data analysis is shown in Figure S4 in the Supporting Information. The highest binding was observed between G4 and HA, and the lowest binding was with heparin (Figure 8). HS and CSA also showed substantial binding to G4, while DS and CSC were lower. The general trend of polyplex mass increases upon GAG solution exposure to G4 polyplexes has the following trend: HA > HS > CSA > CSC > DS > Hep. This binding trend is not well correlated with the trend of GAG charge, continuing to suggest a polyplex–GAG interaction mediated by forces other than electrostatic interactions.

## Discussion

In this work, we have shown that poly(glycoamidoamine) (PGAA) polyplexes interact with glycosaminoglycans (GAGs)

(49) Prevette, L. E.; Kodger, T. E.; Reineke, T. M.; Lynch, M. L. Deciphering the role of hydrogen bonding in enhancing pDNA–polycation interactions. *Langmuir* **2007**, *23* (19), 9773–9784.

in a manner that is not solely charge-dependent and likely in part due to interactions with the carbohydrate moieties on the polymer. However, electrostatic interactions do still play a role in facilitating polyplex interactions with GAGs and triggering uptake into cells. Particularly, GAG sulfation appears to be critical for polyplex internalization by cells, as desulfation with chlorate results in 79–92% reduction in polyplex uptake. This suggests that an electrostatic interaction with sulfate groups is required to bring the polyplex in contact with the cell, and this interaction likely is involved in signaling the endocytic event. Similarly, using GAG-deficient pgsA-745 cells, we observed a dramatic decrease in internalization when the GAGs are not present, suggesting that GAGs serve as primary receptors for cellular internalization of PGAA polyplexes. However, we observe little change in polyplex uptake in HS-deficient cells, suggesting that it is not required for efficient internalization. As HS is the most anionic GAG on mammalian cells, this suggests that GAG charge is not the only factor mediating PGAA polyplex internalization. Gel dissociation assay results imply that PGAA polymers and GAGs may exhibit preferential affinities that can facilitate DNA release in a charge-independent manner. Comparing the gel binding and QCM experiments allows discernment between a binding effect and a dissociative effect. HA revealed the best affinity for binding with G4 polyplexes to form ternary complexes (causes a mass increase in the QCM experiments) while not dissociating the complex at high relative concentration. In contrast, heparin accumulates less on G4 polyplexes (low relative mass increase in the QCM experiments); instead, it dissociates G4 polyplexes readily at lower relative concentrations, which is shown in the gel experiments. High affinity toward ternary complex formation with G4 polyplexes was also observed for HS. High polyplex binding affinity for these GAGs (without polyplex dissociation) is favorable, as HA and HS are nearly ubiquitous in the extracellular matrix and on mammalian cell surfaces, respectively. The polyplexes need to trigger cellular uptake while still remaining intact to protect the nucleic acids from nuclease damage during extra- and intracellular transport. It is interesting that, while HS appears to have high binding affinity for G4, removing HS from cell surfaces does not lead to a substantial decrease in internalization, a facet that is currently not understood and warrants further study in other cell types. However, it is well-known that the cell is a dynamic environment that compensates when certain pathways are modulated. The trend of relative binding affinities measured by QCM corroborates our hypothesis that GAG charge does not solely mediate the interactions between GAGs and polyplexes. Indeed, our group has shown that polymer–pDNA binding occurs partially through hydrogen bonding interactions,<sup>49</sup> so disruption of these interactions could depend on the specific interactions between carbohydrates in the polymer backbone and those in the GAGs.

We have also shown, using TEM, DLS, and  $\zeta$ -potential measurements, that, at lower relative concentrations, the GAGs appear to associate with the surface of the PGAA polyplex without disrupting it. This suggests the ability of

polyplexes to bind closely with the GAGs on the cell surface, possibly recruiting multiple proteoglycans to the polyplex surface. This may be an integral step in internalization, as these close interactions may cause receptor clustering, thereby leading to increased signaling to stimulate endocytosis. Proteoglycans are known to cluster around surface-bound ligands for internalization,<sup>20</sup> a finding which supports particle internalization by this model.

Using the PicoGreen fluorescence recovery assay, we have also shown that GAGs at low relative concentrations can cause structural changes to the PGAA polyplex without fully dissociating the polymer from the pDNA. It is important to note that the concentrations used here are about an order of magnitude lower than that used in the gel electrophoresis assays to study polyplex dissociation. We found that GAGs induce a “loosening” of G4 polyplexes, such that DNA bases are accessible to PicoGreen intercalation (after being forced out by polymer-mediated DNA condensation). This suggests that an overall conformational change may occur upon polyplex binding to cell-surface GAGs. It is also interesting that the results from this assay are directly in line with the results from the QCM experiments, with the exception of HA. This is likely due to our observation that HA forms the tightest ternary complexes, thus G4 polyplex loosening is not observed in the PicoGreen assay. The GAGs are likely internalized in tandem with polyplexes and may assist in DNA release in the endosome, where the polyplex is completely surrounded by GAGs; the engulfment of polyplexes in an endosome increases the local GAG concentration. These interactions, while not strong enough to fully dissociate the complex at low concentrations (encountered upon initial cell surface binding), may represent a key step in DNA release once inside the cell at higher local GAG concentrations (encountered within endosomes).

Results observed with polyplexes containing the T4 polymer were especially interesting. Polyplexes formed with T4 showed higher cellular uptake than the other PGAAAs when GAGs were desulfated with chlorate. Internalization of T4 polyplexes was also higher when GAGs were not present on cells. This suggests that while a GAG-mediated pathway is involved in T4 binding and internalization, T4 polyplexes may be less dependent on these pathways than those which contain the other PGAAAs. These results allow us to begin to understand how differences in hydroxyl number and stereochemistry in the polymer backbone may influence the biological properties of polymeric vehicles.

PGAA interactions with GAGs that lead to efficient internalization appear to be different from other cationic vehicles. We have used linear PEI, a well-studied polymer consisting of repeating ethyleneamine units,<sup>50</sup> for comparison with the PGAA polymers. The data obtained here with PEI

(50) Boussif, O.; Lezoualch, F.; Zanta, M. A.; Mergny, M. D.; Scherman, D.; Demeneix, B.; Behr, J. P. A Versatile Vector for Gene and Oligonucleotide Transfer into Cells in Culture and in vivo - polyethylenimine. *Proc. Natl. Acad. Sci. U.S.A.* **1995**, 92 (16), 7297–7301.



polyplexes suggests that sulfated GAGs may play little or no role in PEI internalization: PEI polyplex uptake actually increases slightly upon GAG desulfation, and PEI polyplexes appear to be internalized by the cell in a GAG-independent manner. It has been suggested that PEI can form nanoscale holes in the plasma membrane, potentially presenting an alternative cell entry mechanism.<sup>51</sup> We have found that nonendocytic internalization of PGAA polyplexes is minimal,<sup>14</sup> and the current study demonstrates that sulfated GAGs on the surface appear to be highly important for their efficient polyplex internalization. These findings illustrate that incorporation of carbohydrate moieties into a PEI-like polyethyleneamine backbone can dramatically impact the biological properties that occur on or within cells, and we have shown that these modifications influence polyplex binding and internalization profiles.

At the surface of the cell, polyplexes likely come into contact with GAGs. The results presented herein suggest that GAG charge is necessary for uptake stimulation, but is not the only factor in polyplex–GAG affinity. Based upon the presented results, we speculate that polyplexes are brought into contact with the cell surface through longer-range charge interactions between the anionic GAG and the cationic polyplex, but tight binding to the GAGs for endocytosis may be facilitated by closer range interactions, such as hydrogen

bonding, between the GAG and polymer carbohydrates. These close-range interactions are likely influenced by the stereochemistry and number of hydroxyl groups in the polymer backbone, as well as the specific carbohydrates in the GAG disaccharide repeat unit. Additional studies to further characterize these interactions and their effects on polyplex trafficking once internalized will further delineate the role of GAGs in PGAA-mediated DNA delivery. These aspects are currently being explored.

**Acknowledgment.** We acknowledge funding of this project from the Beckman Young Investigator Award and the Camille Dreyfus Teacher-Scholar Award Programs, and the Departments of Chemistry at the University of Cincinnati and Virginia Tech for funding of this work. T.M.R. is a fellow of the Alfred P. Sloan Foundation. Thanks to Adam Larkin and Dr. Richie Davis for technical assistance and expert advice in QCM, John McIntosh, Institute for Critical Technologies and Applied Science (ICTAS) at Virginia Tech, for technical assistance in electron microscopy, Dr. Lisa Prevette for assistance in experimental details for polyplex relaxation experiments, and Dr. Nilesh Ingle for performing control experiments. Sincere thanks to Dr. Jeremy Heidel for critical review of the manuscript.

**Supporting Information Available:** Background information on GAGs, competitive inhibition experiments, PicoGreen DNA relaxation experiments, and example QCM traces. This material is available free of charge via the Internet at <http://pubs.acs.org>.

MP100135N

- (51) Hong, S. P.; Leroueil, P. R.; Janus, E. K.; Peters, J. L.; Kober, M. M.; Islam, M. T.; Orr, B. G.; Baker, J. R.; Banaszak Holl, M. M. Interaction of polycationic polymers with supported lipid bilayers and cells: Nanoscale hole formation and enhanced membrane permeability. *Bioconjugate Chem.* **2006**, *17* (3), 728–734.